Supporting Information for

ORIGINAL ARTICLE

Cancer-cell-biomimetic nanoparticles systemically eliminate hypoxia tumors by synergistic chemotherapy and checkpoint blockade immunotherapy

Yongrong Yao, Huachao Chen*, Ninghua Tan*

State Key Laboratory of Natural Medicines, School of Traditional Chinese Pharmacy, China Pharmaceutical University, Nanjing 211198, China

Received 11 July 2021; received in revised form 27 September 2021; accepted 4 October 2021

*Corresponding authors. Tel.: +86 21 86185772 (Ninghua Tan); +86 21 86185772 (Huachao Chen).

E-mail addresses: nhtan@cpu.edu.cn (Ninghua Tan), huachao.chen@cpu.edu.cn (Huachao Chen).

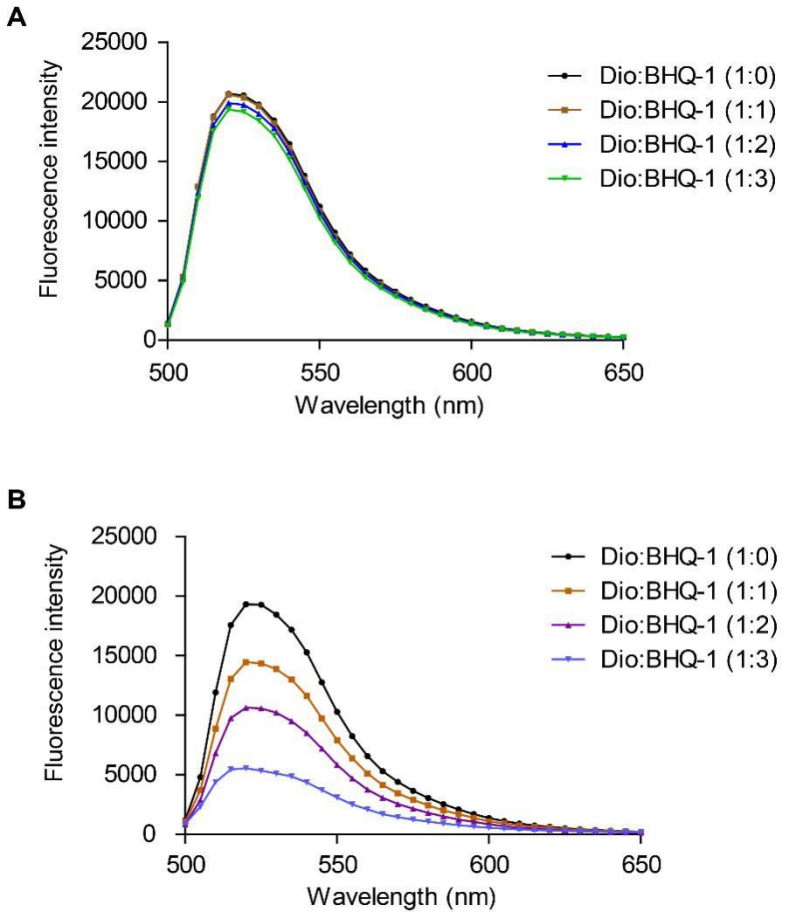

Figure S1 Investigation of fluorescence resonance energy transfer (FRET) in BMS/RA@CC-Liposome. (A) The changes of fluorescence intensity of BMS/RA@CC-Liposome (Dio labelled membrane, BHQ-1 doped in shells of liposome), along with increasing proportions of BHQ-1; (B) The changes of fluorescence intensity of BMS/RA@CC-Liposome (Dio and BHQ-1 both doped in shells of liposome), along with increasing proportions of BHQ-1.

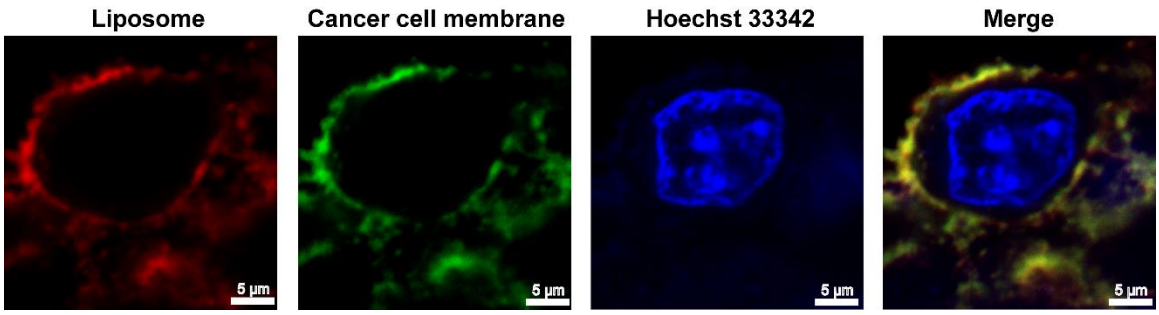

Figure S2 Colocalization of liposome and cancer cell membrane upon cellular uptake. BMS/RA@CC-Liposome was synthesized with liposome loaded with Cy5.5 (red channel) and cancer cell membrane labeled with Dio (green channel). Scale bar=5 μm.

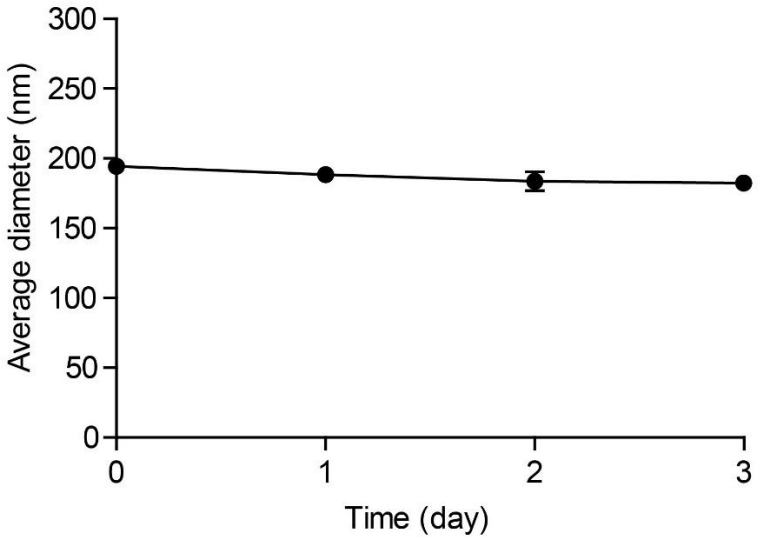

Figure S3 The stability of BMS/RA@CC-Liposome. The stability study of BMS/RA@CC-Liposome was evaluated at 37 ℃ during three days. Data are given as mean ±SD (*n*=3).

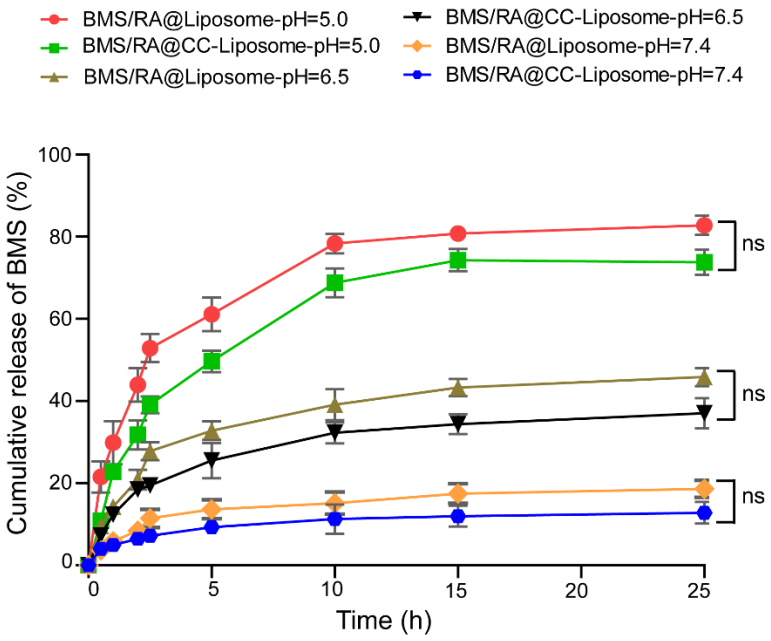

Figure S4 *In vitro* release profiles of BMS. The release profiles of BMS of BMS/RA@Liposome and BMS/RA@CC-Liposome were performed at pH 5.0, 6.5 and 7.4. Data are given as mean±SD (*n*=3). ns, not significant.

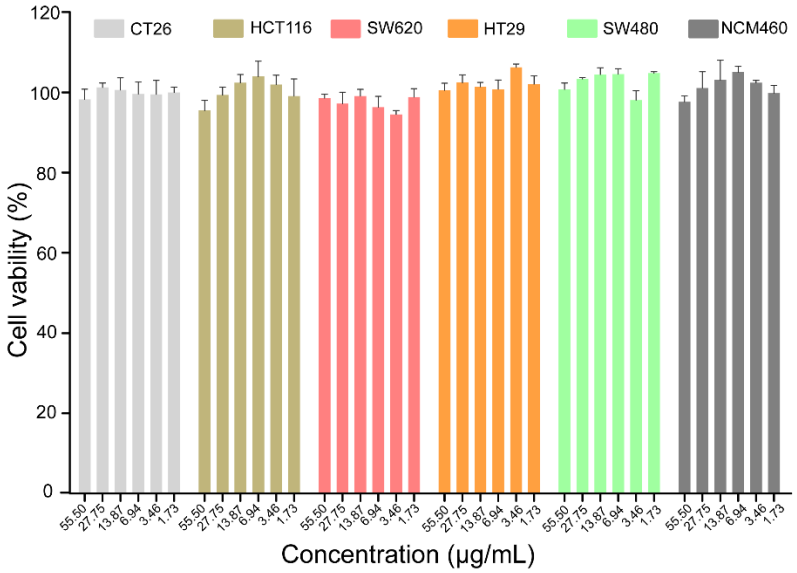

Figure S5 SRB assay of different colon cancer cells and normal cells after CC-Liposome treatment. CT26, HCT116, SW620, HT29, SW480 and NCM460 cells in the presence of a series of

CC-Liposome (at doses of 55.5, 27.75, 13.87, 6.94, 3.46, and 1.73 μg/mL cancer cell membrane) concentrations for 48 h incubation. Data are given as mean ±SD (*n*=3).

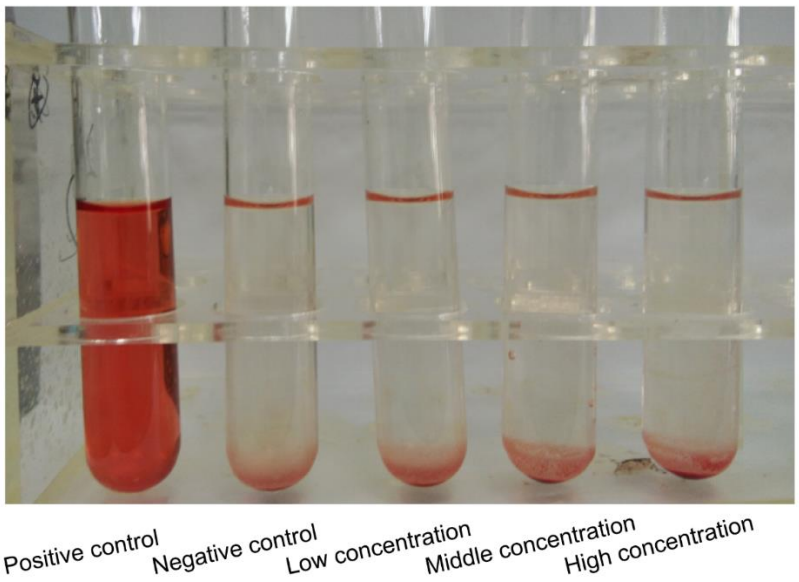

Low concentration (13.87 μg/mL)	Middle concentration (27.75 μg/mL)	High concentration (55.50 μg/mL)
-0.007354969	9.19371E-05	-0.001838742
-0.007079158	9.19371E-05	-0.001838742
-0.007354969	9.19371E-05	-0.002114554

Figure S6 Hemolytic test of CC-Liposome with three concentrations in red blood cell of rabbit. The red blood cells of rabbit were added different concentrations of CC-Liposome, standing for 3 h at 37 ℃ before measuring. Data are given as mean ±SD (*n*=3).

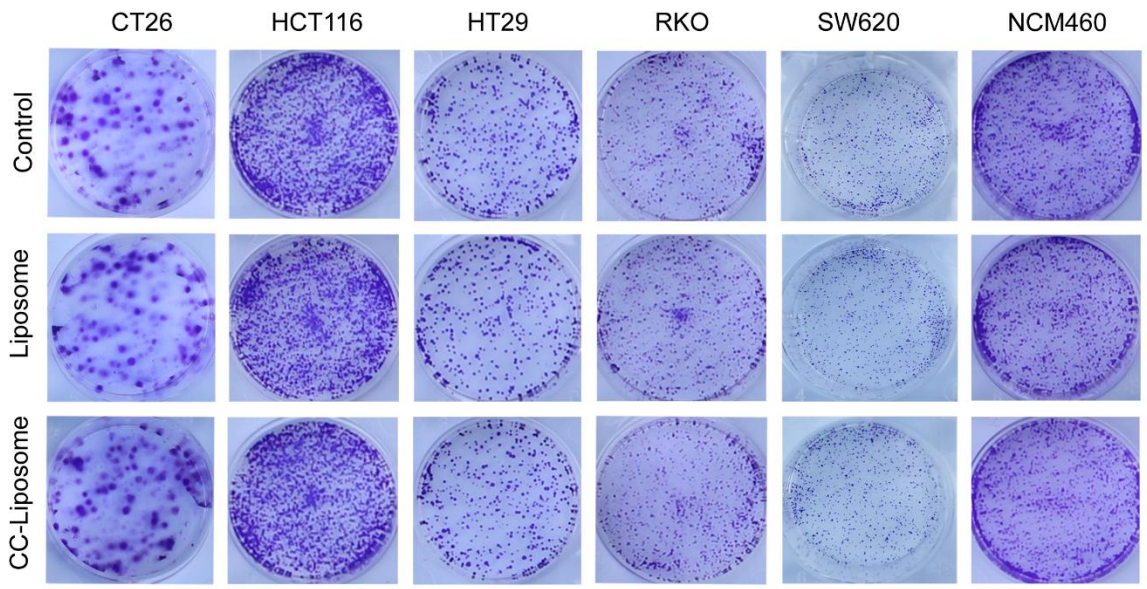

Figure S7 The effect of CC-Liposome and Liposome on colony formation activity in different cells. CT26, HCT116, HT29, RKO, SW620 and NCM460 cells in the presence of Liposome and CC-Liposome for 48 h incubation.

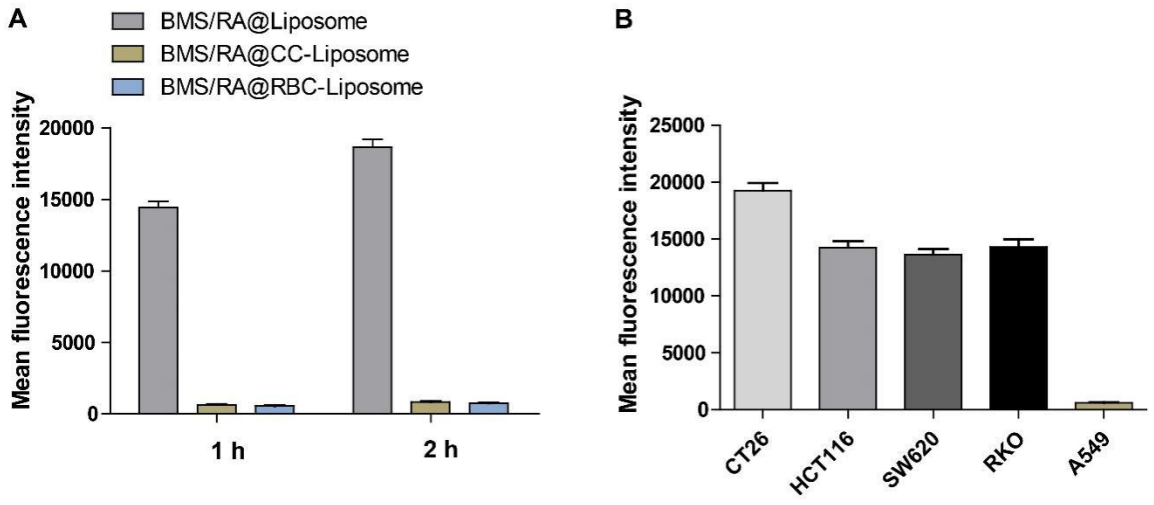

Figure S8 Quantification of flow cytometer analysis. (A) Quantitative flow cytometry analysis of intracellular uptake of BMS/RA@Liposome, BMS/RA@CC-Liposome and BMS/RA@RBC-Liposome in RAW264.7 cells after 1-2 h incubation. Data are given as mean ±SD (*n*=3). (B) Quantitative flow cytometry analysis of BMS/RA@CC-Liposome uptake with CT26, HCT116, SW620, RKO and A549 cells. Data are given as mean ±SD (*n*=3).

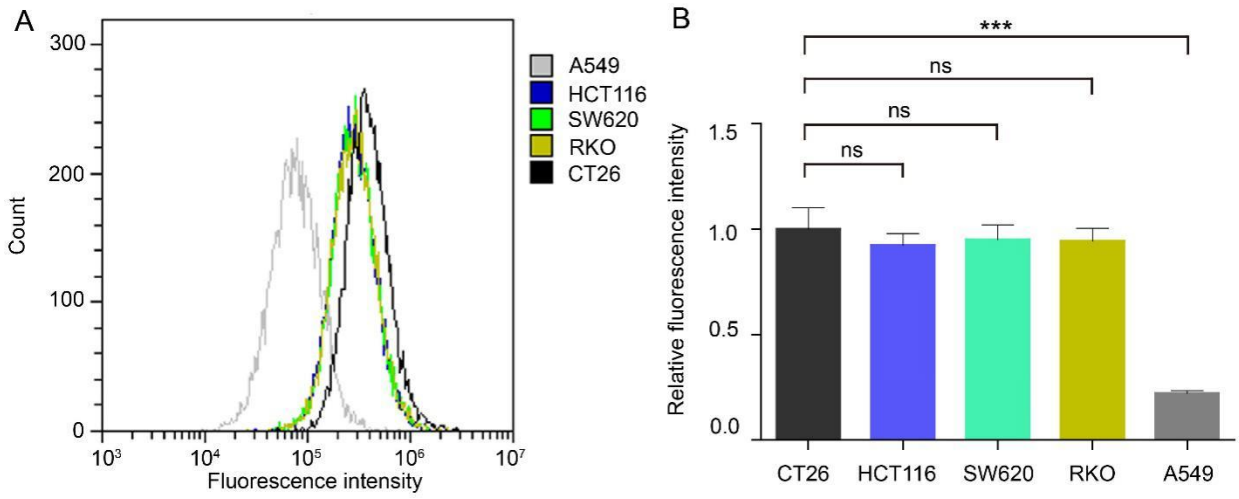

Figure S9 Intracellular uptake of BMS/RA@CC-Liposome in CT26, HCT116, SW620, RKO and A549 cells after 2 h incubation. (A) Flow cytometer analysis of BMS/RA@CC-Liposome in CT26, HCT116, SW620, RKO and A549 cells; (B) Quantitative flow cytometry analysis of (A). Data are given as mean ±SD (n=3). ***P<0.001. ns, not significant.

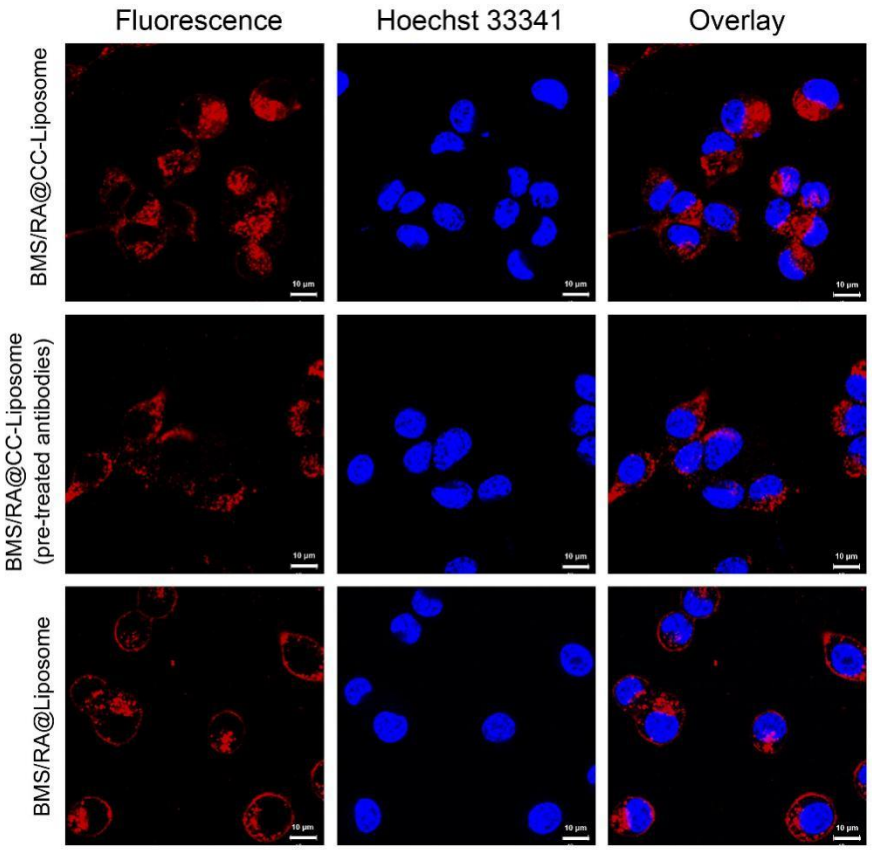

Figure S10 Investigation of cellular uptake mechanism of BMS/RA@CC-Liposome. Confocal fluorescence imaging of CT26 cells incubated with the BMS/RA@CC-Liposome for 3 h; CT26 cells pretreated with excessive free TF-antigen antibody and E-cadherin antibody, followed by incubation with the BMS/RA@CC-Liposome for 3 h; CT26 cells incubated with BMS/RA@Liposome for 3 h. Scale bars=10 μm.

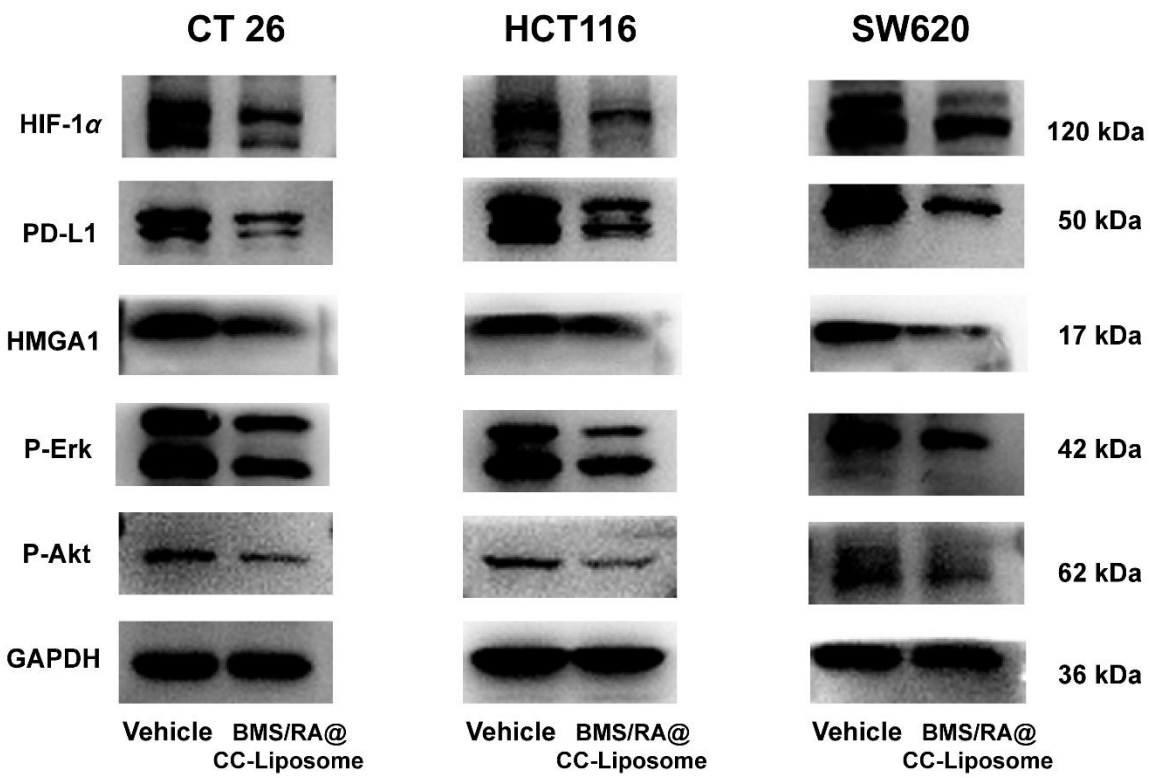

Figure S11 Investigation of the effect of BMS/RA@CC-Liposome on the relative proteins expression in colon cancer cells. Western blotting analysis for the expression of HIF-1α, PD-L1, HMGA1, P-Erk and P-Akt expression in CT26, HCT116 and SW620 cells after BMS/RA@CC-Liposome treatment (at dose of 100 nmol/L RA-V).

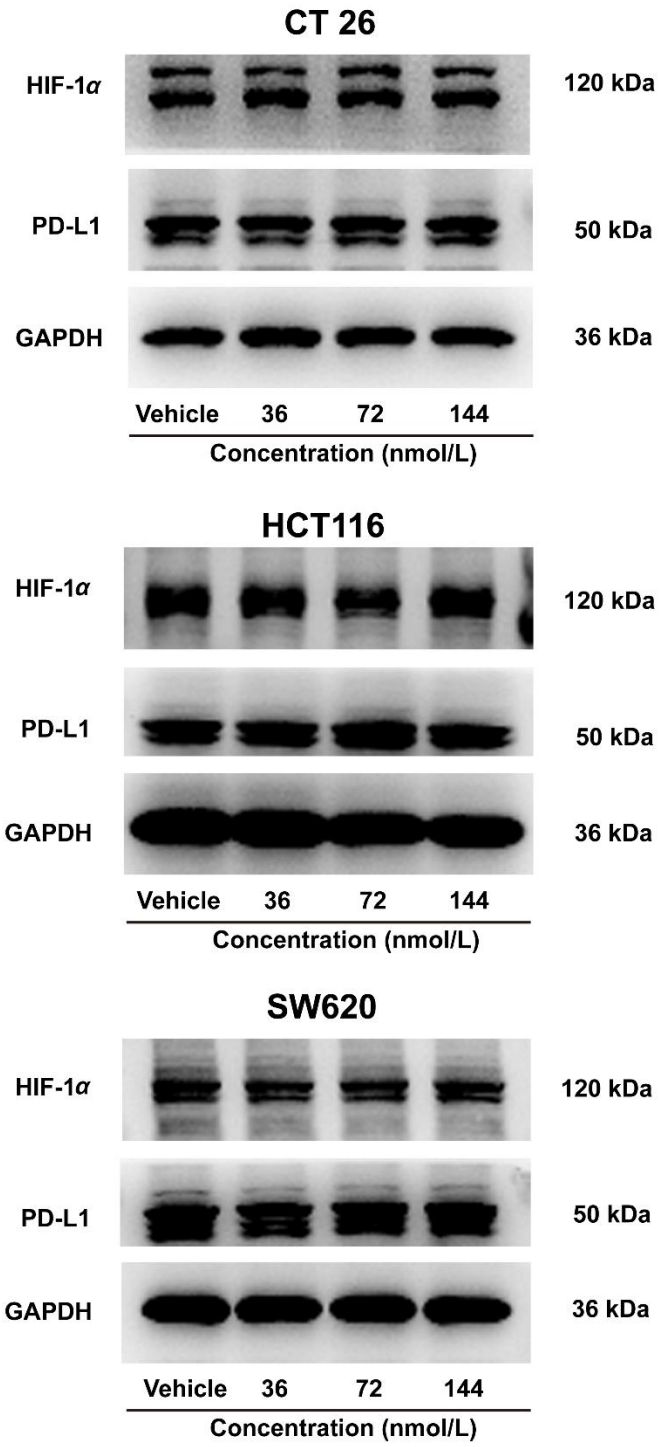

Figure S12 Investigation of the effect of BMS on HIF-1α, PD-L1 expression in colon cancer cells. Western blotting analysis for the expression of HIF-1α and PD-L1 expression in CT26, HCT116 and SW620 cells after BMS treatment.

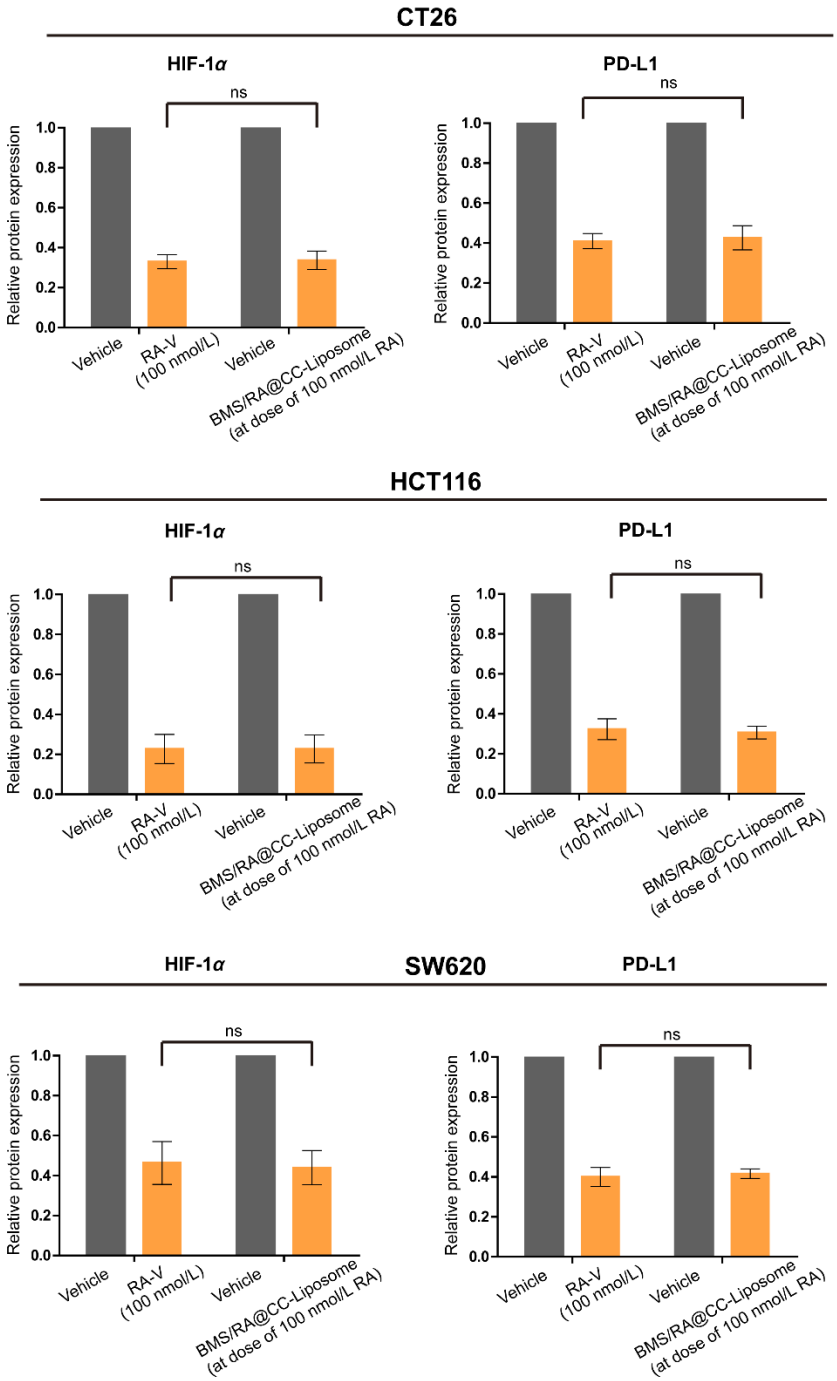

Figure S13 Quantitative analysis of the expression of HIF-1*α* and PD-L1. Quantitative analysis of the expression of HIF-1*α* and PD-L1 at dose of 100 nmol/L RA-V treatment in Fig. 4A, 4D, 4E and BMS/RA@CC-Liposome treatment (at dose of 100 nmol/L RA-V) in Fig. S11 by optical densitometry using Image J. Data are given as mean ±SD (*n*=3). ns, not significant.

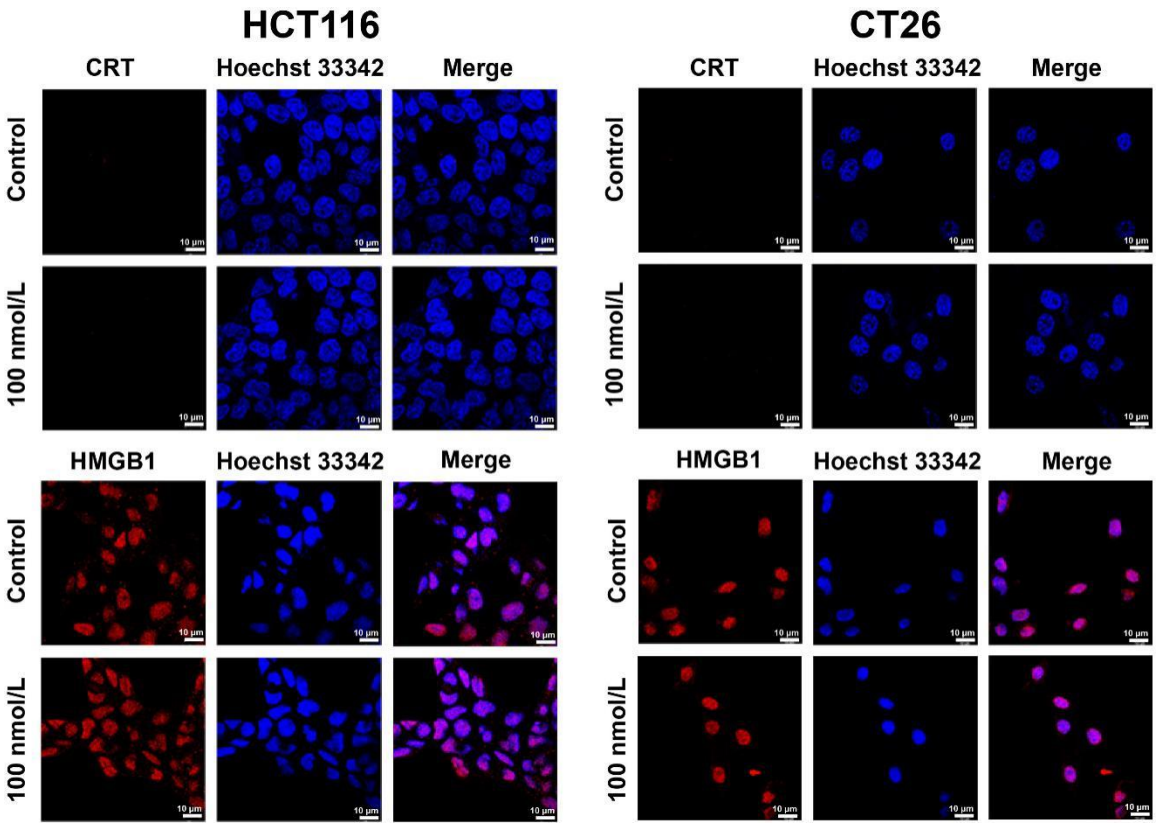

Figure S14 Immunofluorescence assay of calreticulin (CRT) and high-mobility group box 1 (HMGB1). HCT116 and CT26 cells were treated with RA-V at dose of 100 nmol/L, then stained with CRT and HMGB 1, respectively. The nucleus was stained with Hoechst 33342 (blue). The CRT and HMGB1 proteins were labeled with Alexa 555 (red). Scale bar=10 μm.

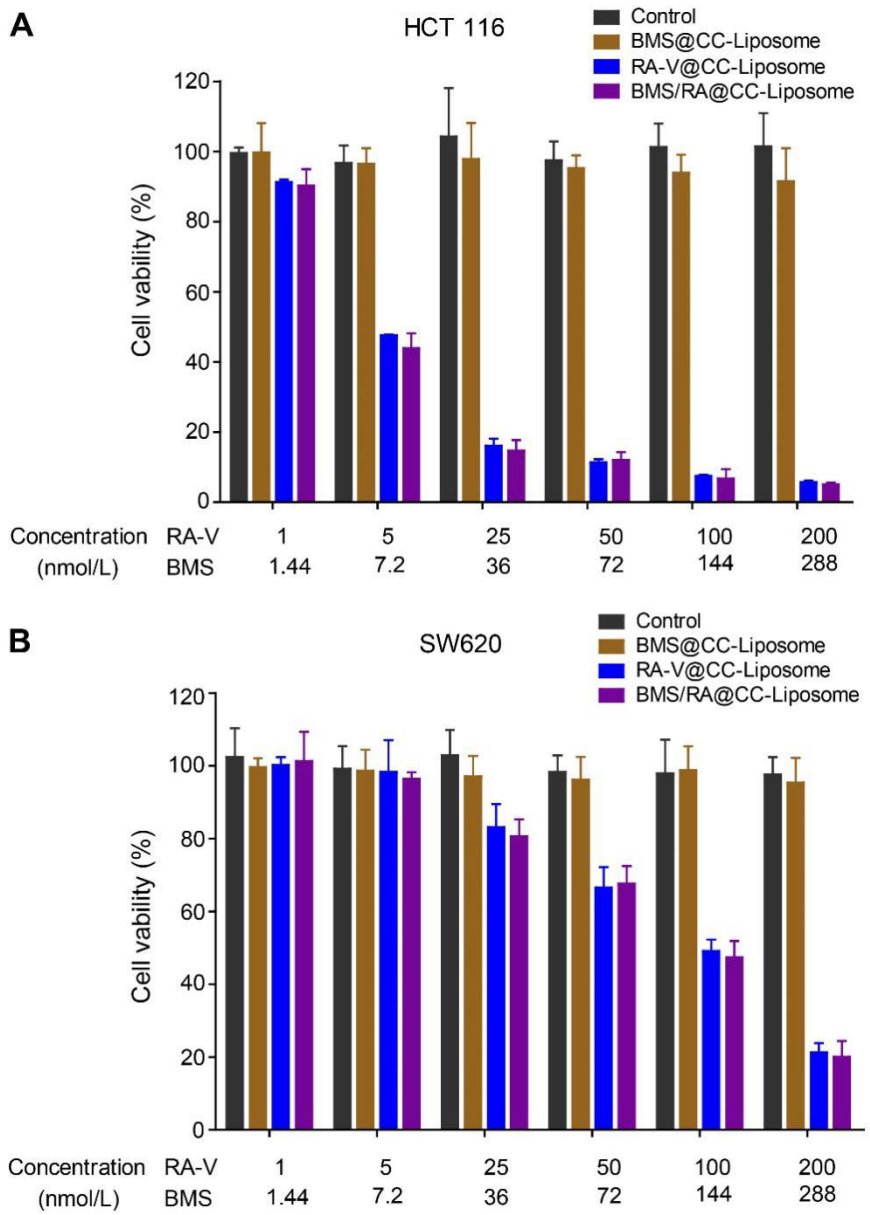

Figure S15 SRB assay of HCT116 cells and SW620 cells after different treatments. (A) SRB assay of HCT116 in the presence of BMS@CC-Liposome, RA-V@CC-Liposome, and BMS/RA@CC-Liposome. Data are given as mean ±SD (*n*=3). (B) SRB assay of SW620 cells in the presence of BMS@CC-Liposome, RA-V@CC-Liposome, and BMS/RA@CC-Liposome. Data are given as mean ±SD (*n*=3).

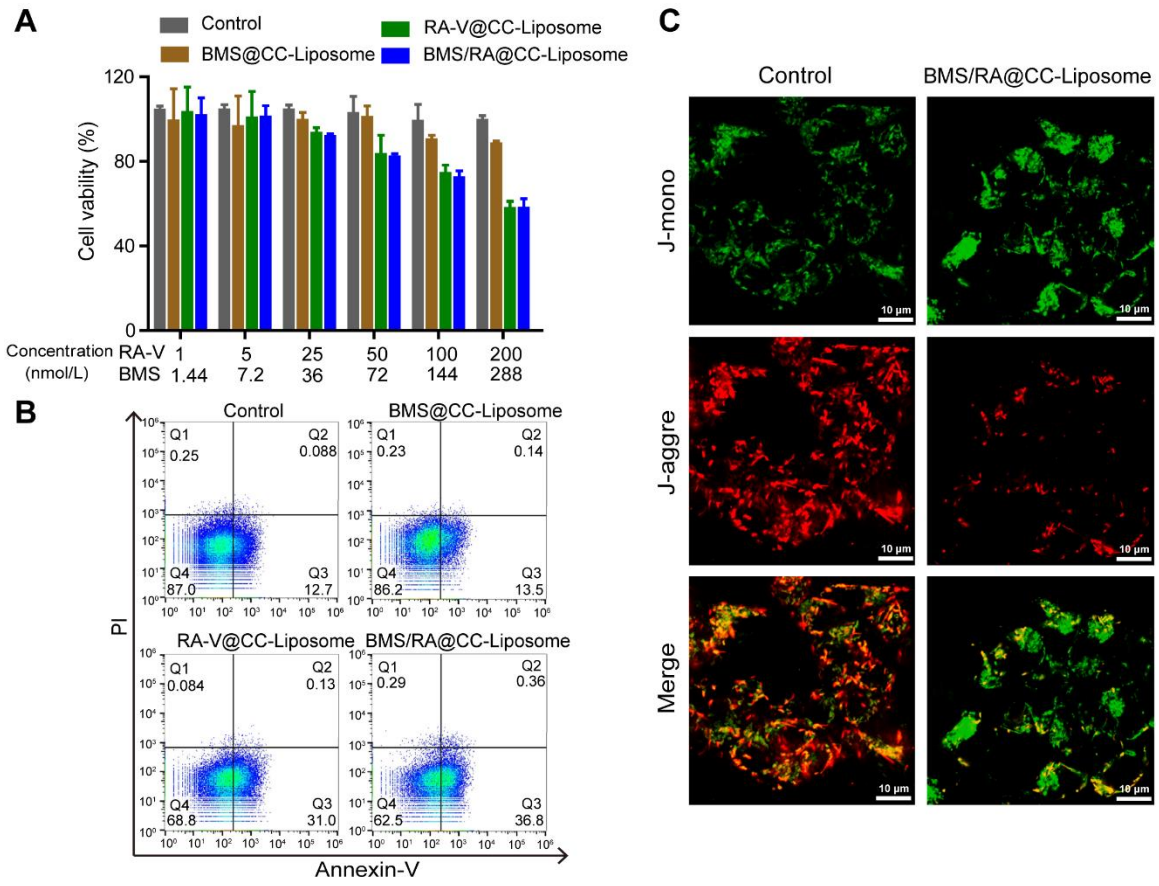

Figure S16 Analysis of CT26 cell after different treatments. (A) SRB assay of CT26 cells in the presence of BMS@CC-Liposome, RA-V@CC-Liposome, and BMS/RA@CC-Liposome. Data are given as mean ±SD (*n*=3). (B) Flow cytometric analysis of CT26 cells death with different treatments; (C) Confocal fluorescence images in CT26 cells treated with PBS and BMS/RA@CC-Liposome. Scale bars=10 μm.

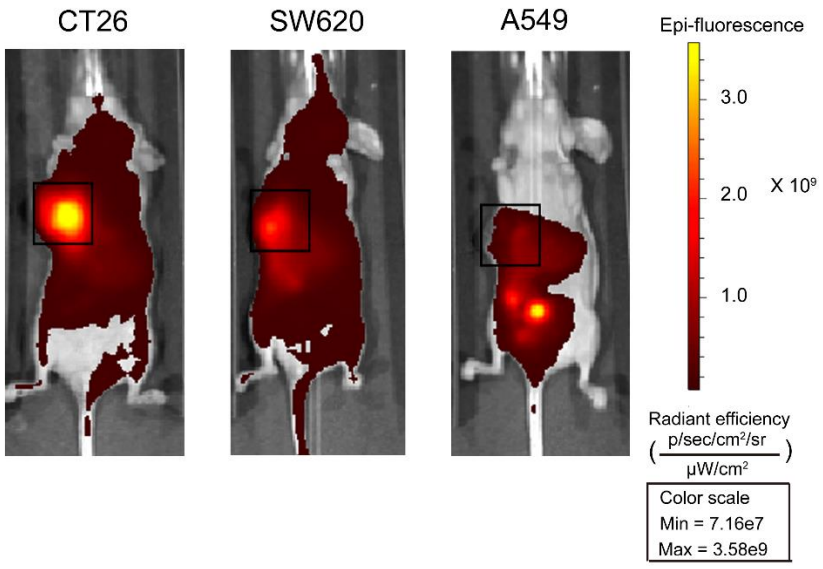

Figure S17 Investigation of the homing specificity in different mice models. *In vivo* images of mice after tail vein injection of BMS/RA@CC-Liposome at 12 h in CT26, SW620 and A549 tumor-bearing mice, respectively.

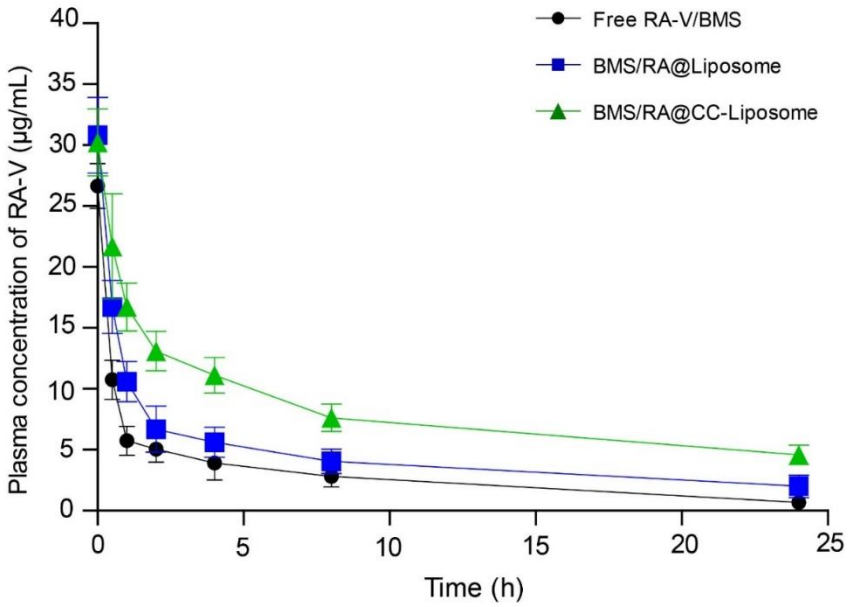

Figure. S18 Plasma concentration-time curves of RA-V. Determinations of RA-V from Free RA-V/BMS-202, BMS/RA@Liposome and BMS/RA@CC-Liposome after intravenous injection in mice. Data are given as mean ±SD (*n*=3).

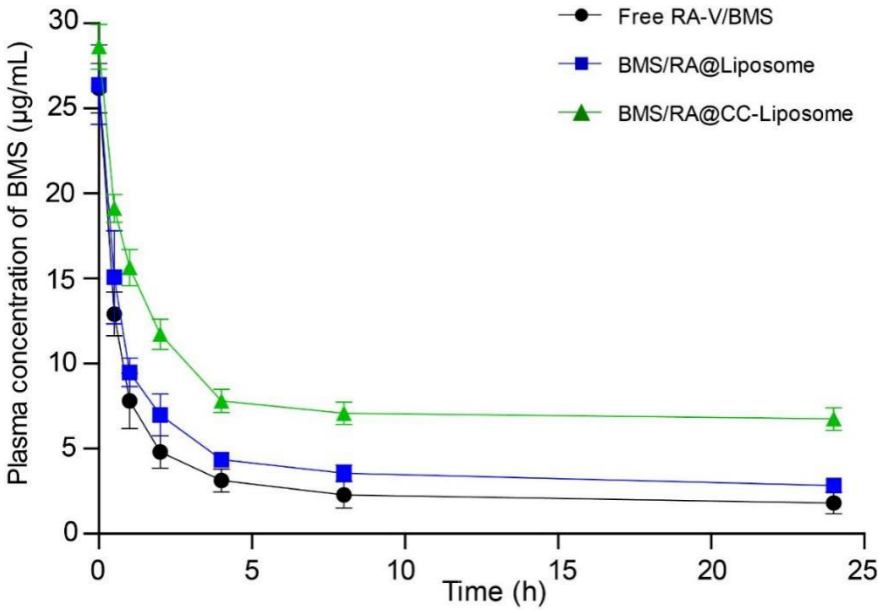

Figure. S19 Plasma concentration-time curves of BMS. Determinations of BMS from Free RA-V/BMS-202, BMS/RA@Liposome and BMS/RA@CC-Liposome after intravenous injection in mice. Data are given as mean ±SD (*n*=3).

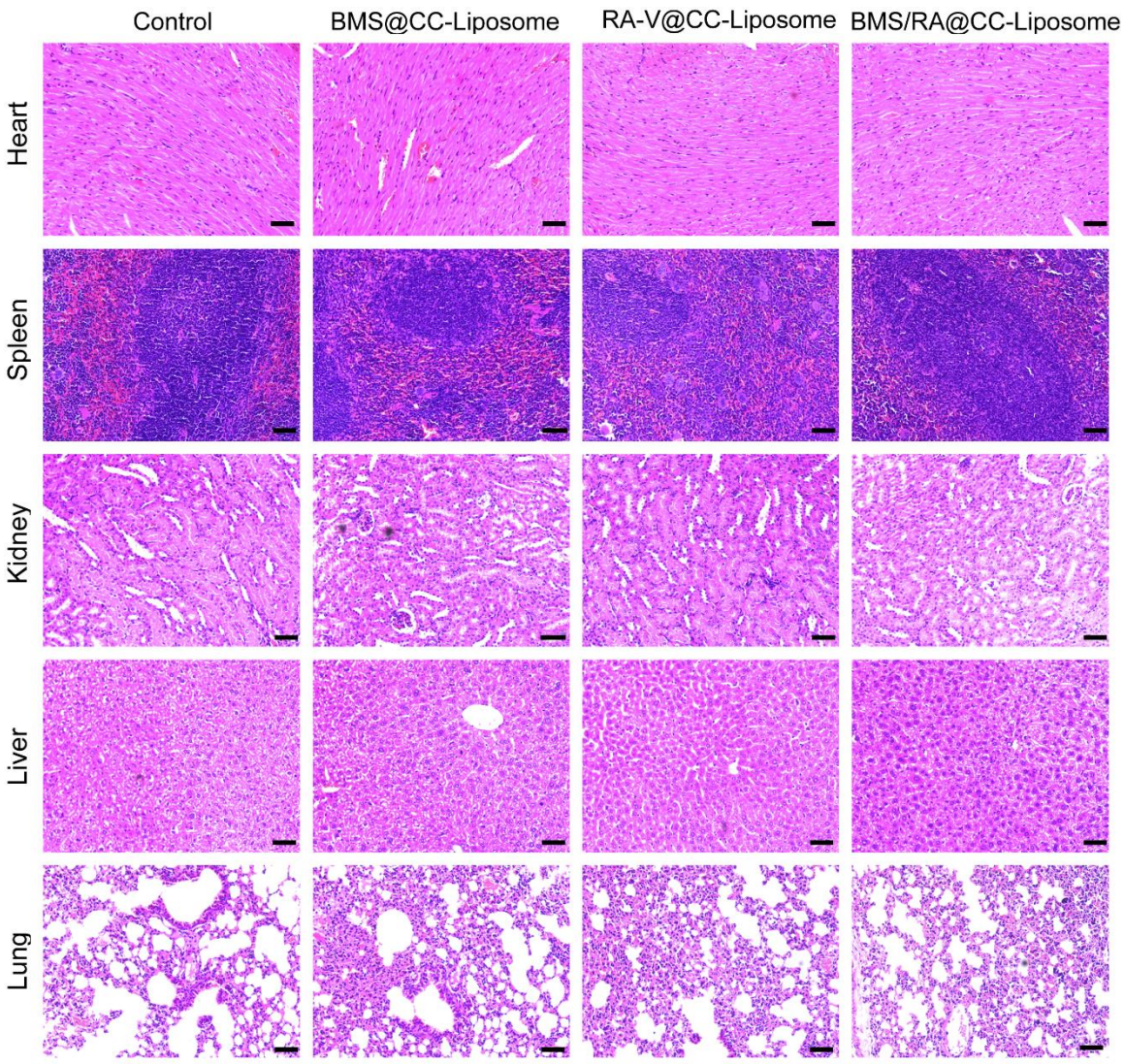

Figure S20 H&E stained images of major organs for *in vivo* toxicity assay. Histological observation of the organs collected from CT26 tumor-bearing BALB/c mice after different treatments. Scale bar=50 μm.

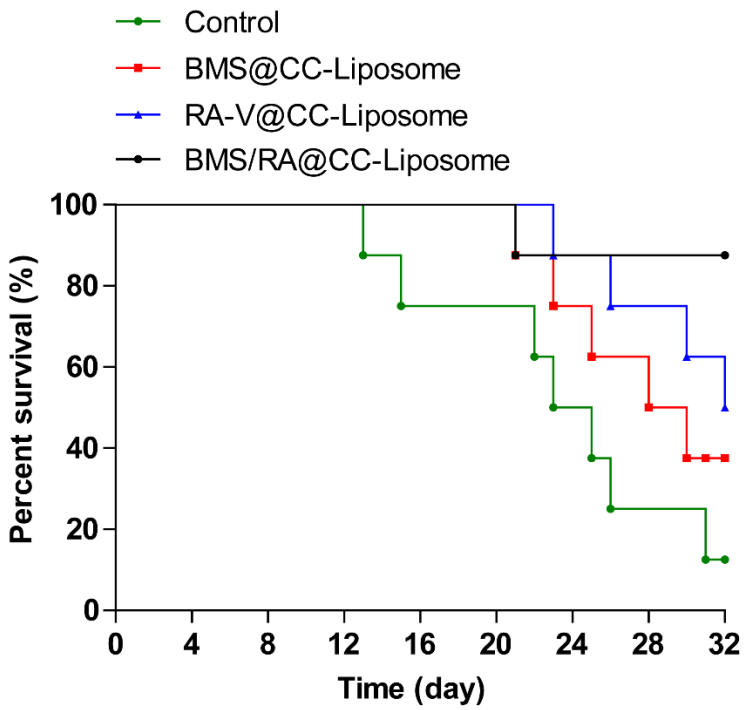

Figure S21 Survival rates of CT26 tumor-bearing mice during 32 days. CT26 tumor-bearing mice with different treatments indicated were recorded survival rates (*n*=8).